Preprints.org

Article

Not peer-reviewed version

Enhancing Sustainability: Brewer's Spent Grain-based Biochar as a Renewable Energy Source and Agriculture Substrate

Romina Zabaleta , Erick Torres , Eliana Sanchez , Rodrigo Torres-Sciancalepore , María Paula Fabani , Germán Mazza , Rosa Rodriguez *

Posted Date: 8 July 2024

doi: 10.20944/preprints202407.0589.v1

Keywords: brewer’s spent grain biochar; pyrolysis temperature; bioenergy indices; germination test

Preprints.org is a free multidiscipline platform providing preprint service that is dedicated to making early versions of research outputs permanently available and citable. Preprints posted at Preprints.org appear in Web of Science, Crossref, Google Scholar, Scilit, Europe PMC.

Copyright: This is an open access article distributed under the Creative Commons Attribution License which permits unrestricted use, distribution, and reproduction in any medium, provided the original work is properly cited.

Preprints.org (www.preprints.org) | NOT PEER-REVIEWED | Posted: 8 July 2024 doi:10.20944/preprints202407.0589.v1

Disclaimer/Publisher's Note: The statements, opinions, and data contained in all publications are solely those of the individual author(s) and contributor(s) and not of MDPI and/or the editor(s). MDPI and/or the editor(s) disclaim responsibility for any injury to people or property resulting from any ideas, methods, instructions, or products referred to in the content.

Article

Enhancing Sustainability: Brewer's Spent Grain-Based Biochar as a Renewable Energy Source and Agriculture Substrate

Romina Zabaleta [1], Erick Torres [1], Eliana Sánchez [1], Rodrigo Torres-Sciancalepore [2], María Paula Fabani [1,3], Germán Mazza [2] and Rosa Rodriguez [1,*]

[1] Instituto de Ingeniería Química-Grupo Vinculado al PROBIEN (CONICET-UNCO), Facultad de Ingeniería, Universidad Nacional de San Juan, Argentina
[2] Instituto de Investigación y Desarrollo en Ingeniería de Procesos, Biotecnología y Energías Alternativas, PROBIEN (CONICET-UNCo), Neuquén, Argentina
[3] Instituto de Biotecnología, Facultad de Ingeniería, Universidad Nacional de San Juan, Argentina
* Correspondence: rrodri@unsj.edu.ar

Abstract: This study investigates the influence of pyrolysis temperature on the main properties of BSG (brewer's spent grain) biochar and evaluates its suitability as an energy vector and as a substrate component. Pyrolysis tests were carried out at 673, 773, and 873 K. Bioenergy indexes were calculated for BSG and its biochar, and germination tests were carried out to obtain lentil sprouts. The results showed that the BSG biochar obtained at the lowest temperature biochar presented the best performance for use as biofuel. Regarding the germination tests, the different biochars were applied at 4 doses, and the evaluated parameters such as germination percentage, germination rate, mean germination time, and seed vigor were strongly influenced by the biochar addition. The biochar at 773 K added at a dose of 5% doubled the values of mean germination time, seed vigor, and time for 50% of the seeds to emerge compared to the control, constituted only with distilled water. The sustainable BSG valorization through pyrolysis reduces waste and contributes to circular economy practices by transforming industrial by-products into valuable resources for energy and agriculture. This approach highlights the importance of sustainability in reducing the environmental impact of industrial waste and promoting renewable energy sources.

Keywords: brewer's spent grain biochar; pyrolysis temperature; bioenergy indices; germination test

1. Introduction

Beer is the most widespread alcoholic beverage, and the third most consumed beverage in the world [1], and the brewer's spent grain (BSG) from beer production is the first by-product generated [2]. In recent years, the number of microbreweries in Argentina has increased substantially in response to the growing demand for craft beer, an alternative to traditional beer that has been widely accepted by the local market.

Argentina has an installed capacity of 23.9 million hectoliters of beer, producing about 20 million hectoliters per year, whose main raw material is malted barley [3]. The BSG is the main waste generated by the brewery industry, representing 85% of the total process waste [4]. This solid lignocellulosic waste is generated after the mashing of malted barley, where the starch is converted into fermentable sugars by the addition of water and, then BSG is separated from the malted barley wort by filtration. BSG composition is characterized by being rich in protein (15-25% on a dry basis) and fiber (around 70% on a dry basis) and also contains different vitamins (especially those of the B complex: thiamine, riboflavin, niacin, pantothenic acid, pyridoxine, biotin, and folic acid) [5], therefore different works focus on its incorporation in the human diet [6].

© 2024 by the author(s). Distributed under a Creative Commons CC BY license.

Preprints.org (www.preprints.org) | NOT PEER-REVIEWED | Posted: 8 July 2024 doi:10.20944/preprints202407.0589.v1

Although the BSG has several applications [7–9], due to the large amount that is generated, it is necessary to find new applications that also promote a circular economy. Biochar production is therefore an alternative that should be explored to find new opportunities for converting such waste into carbon-based materials.

Through pyrolysis, it is possible to produce different biofuels such as gas, bio-oil, and biochar. In all cases, the biomass usually is densified considering the calorific value of the bio-waste and three products [10]. In this thermochemical process, the temperature is one of the variables affecting the physicochemical characteristics of biochar [11]. To obtain a higher yield of biochar than other by-products, relatively low temperatures are required, due to the carbonization reactions [12]. Other important variables that modify the product distribution in pyrolysis and their characteristics are the particle size of the sample, the nitrogen flow rate used to remove the air from the reactor used, the gas and solid residence time, and the process heating rate [13,14]. Biochar has several uses such as energy vector, amendment soil, substrate in soilless cultivation, and additive on composite materials, among others [15,16]. At the same time, the chemical and physical properties of biochar depend largely on the biomass and the operating conditions of the process [11].

Considering the biochar use as an energy vector, it is possible to evaluate the potential of biofuels (e.g., biomass or biochar) for heat generation, by using bioenergy indices that allow comparing their energetic characteristics with those of classical fossil fuels and also, with other biofuels [17]. In addition, it has been shown that biochar can be used as a substrate for the cultivation of various vegetables [18], with the production of sprouts being an alternative crop that has gained importance in human diets, as well as fodders in animal feed, since sprouts have a nutritional quality superior to dry cereals, with a high content of proteins, vitamins, and bioactive compounds [19,20].

Given the versatility of this bio-waste, it has recently regained interest. Dessì et al. [21] studied the triplet kinetics and reaction mechanism of pyrolysis, determining a multistage reaction model for its thermal valorization. Likewise, Sobek et al. [22] analyzed the kinetic mechanism of pyrolysis with a focus on the recovery of phenolic compounds and fatty acids. Ashman et al. [23] proposed an integrated biorefinery through the addition of catalysis precursor in BSG biomass, to improve biofuel components, in addition to producing bio-template silver particles. On the other hand, a review by Jo-vine et al. [24] discusses in depth the use of BSG to obtain biogas and consequently reduce the use of fossil fuels. Olszewiski et al. [25] and De Araújo et al. [26] studied the hydrothermal carbonization of the same bio-waste, the first emphasizing the pretreatment while the latter studied its activation and its application to treat wastewater.

Although BSG has been studied and reviewed extensively, little is known about the pyrolysis temperature effect of bio-waste and its application as a biofuel and substrate constituent. Hence, this current study explores sustainable alternatives for its valorization considering its use as an energy vector and substrate for sprout production. Therefore, first, a comprehensive characterization of BSG and its biochar produced by slow pyrolysis at 673, 773, and 873 K was carried out, considering proximate analysis (for moisture, volatile matter (VM), fixed carbon, and ash contents) and elemental analysis (carbon (C), hydrogen (H), nitrogen (N), oxygen (O), and sulfur (S) contents) together with the higher heating value (HHV). In addition, Fourier Transform Infrared (FTIR) spectroscopy was applied to identify BSG biochar chemical bonds, and the methods of Brunauer- Emmett- Teller (BET) specific surface area, Scanning Electron Microscopy (SEM) and Energy Dispersive X-ray Spectroscopy (EDS) were implemented for the study of BSG biochar surface. Four bioenergy indices were then calculated to compare BSG and its biochar with classical fossil fuels. Finally, the BSG biochar obtained at each temperature was assessed using germination assay to establish its application as a substrate constituent and to produce sprout. A logic diagram of this research is presented in Figure 1.

Preprints.org (www.preprints.org) | NOT PEER-REVIEWED | Posted: 8 July 2024 doi:10.20944/preprints202407.0589.v1

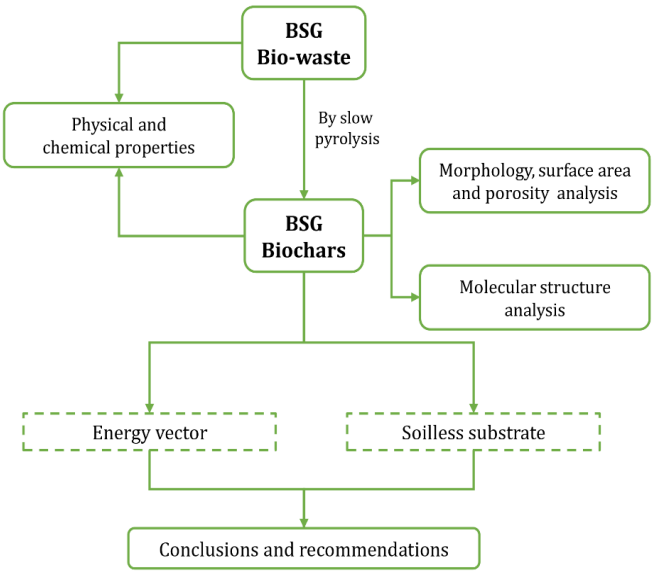

Figure 1. Logic diagram of work.

2. Materials and Methods

2.1. Bio-Waste Characterization

In this work, BSG was used as pyrolysis feedstock. The BSG was acquired from "Cumbre" brewery, located in San Juan Province, Argentina.

To transform the BSG using the slow pyrolysis process, it is necessary to dry it up to a humidity of less than 10%, (initial moisture: 60-80%), according to Maqhuzu et al. [27] and Capossio et al. [28]. Proximate analysis (moisture, ash, and VM) was determined according to ASTM standards (ASTM E872-82 and ASTM D1102-84) [29,30], and ultimate analysis was performed using an elemental analyzer (AuroEA3000). The higher heating value (HHV) was calculated according to the work of Lorente et al. [31]. The apparent density of BSG was determined following the ASTM standards (ASTM E873-82) [32]. The pH and electrical conductivity (EC) were determined in a suspension of biochar in distilled water at a ratio of 1:10 (w/v) as recommended by Bu et al. [33].

2.2. Pyrolysis Experiments for Biochar Production

The experiments were carried out in a cylindrical reactor as described by Rodriguez-Ortiz et al. [11]. The reactor had a capacity of 4 kg of feedstock. The dried BSG samples were introduced to the reactor with a moisture content of 6% by weight. The energy to heat the reactor was supplied by an electrical resistance with a power of approximately 2000 W. The thermochemical process occurs under an inert atmosphere (N_2 atmosphere) at temperatures equal to 673, 773, and 873 K, with a residence time of 2 hours [34,35]. To evaluate only the influence of temperature on the biochar characteristics, the BSG was introduced into the reactor when it reached the desired temperature.

2.3. Physical and Chemical Properties of the Biochar

The proximate analysis and HHV, as well as apparent density, pH, and EC, were determined following the procedures described in Section 2.1. BSG biochar yield on a dry basis was calculated as described by De Araújo et al. [26]. In addition, carbon retention, water holding capacity (WHC), stable C mass fraction, aromaticity factor, recalcitrance potential, and carbon sequestration potential for BSG biochars were calculated using Equations (S1)–(S6) shown in the Supplementary Materials.

The biochar FTIR spectra were acquired by an Infralum FT-08 FTIR spectrometer using the KBr pressed pellet method. All spectra were collected at room temperature using 60 scans in the range of 4000-400 1/cm. SEM-EDS analysis (carried out by the Laboratory for Analysis of Materials by X-ray Spectrometry, Cordoba University, Argentina) was carried out to observe the microscopic structures

Preprints.org (www.preprints.org) | NOT PEER-REVIEWED | Posted: 8 July 2024 doi:10.20944/preprints202407.0589.v1

of BSG and to identify different elements present in it. A scanning electron microscope (SEM-EDS, EVO MA10W, Carl Zeiss) with a Bruker X-ray energy dispersion (EDS) microanalysis system (Quantax 200) and an SDD XFlash 6/30 analytical detector were employed. Textural characteristics were performed by nitrogen adsorption isotherms, obtained at 77 K (boiling point of nitrogen) using Micromeritics Sortometer (ASAP 2050, America). The specific surface area and pore volume were determined by the Brunauer–Emmet–Teller (BET) method.

2.4. Bioenergy Indices for BSG and BSG Biochar

The bioenergy indices provide a characterization of biomass and biochar in energy terms. They allow evaluate the calorific value in terms of energy density, the capacity of biomass and biochar as biofuel, and CO_2 emission compared to fossil fuels [36].

The indices calculated were the bioenergy density (BD), which is an indicator of the energy released during incomplete combustion per unit volume of biofuel [17]; the fuel value index (FVI), which expresses the fuel potential of biofuel in terms of flammability and heat generation, this depends on the low heat value (LHV), ash content, and apparent density in the samples [36]. The fossil fuel equivalent volume (FFEV), an equivalence index, provides information on the volume, expressed in liters, of fossil fuel, required to produce the same amount of energy as a cubic meter of biofuel [37]. FFEV depends on the association between biofuel BD and fossil fuel BD [36]. Finally, the potential CO_2 retention (PCOR), calculates the mass of CO_2 released from combustion that could potentially be suppressed by replacing certain fossil fuels with their equivalent in biofuel [27,38]. These bioenergy indices were presented in Equations (S7)–(S14) in the Supplementary Materials.

2.5. Germination Assay and Growth Seedling

To evaluate the effect of biochar on germination seeds and growing seedlings, germination tests were carried out according to the methodology proposed by Ali et al. [39]. Each biochar (obtained at three temperatures 673, 773, and 873 K) was added in Petri dishes at different doses of 0, 0.5, 1.0, 2.5, and 5.0 g/Petri dishes and 20 mL of water, corresponding to 0, 10, 20, 50, and 100 t/ha on a volume basis at 10 cm soil depth or 0%, 1%, 2%, 5%, and 10%, respectively [40]. Fifteen seeds of the lens (*Lens culinaris* var. *vulgaris*) were sown in Petri dishes. Seed germination percentage (GP), germination rate (GR), mean emergence time (MET), and seed vigor (SV) were calculated as follows equations:

$$\text{Germination Percentage (GP)} = \left(\frac{SNG}{SN0}\right) \cdot 100 \quad (1)$$

SNG and SN0 are germinated seeds in the total and the total number of viable seeds, respectively [41].

$$\text{Germination Rate (GR)} = \frac{\sum N}{\sum (n \cdot g)} \quad (2)$$

N is the number of germinated seeds; n is the seeds germinated on growth day and g is the total number of germinated seeds.

$$\text{Mean Emergence Time (MET)} = \frac{\sum Dn}{\sum n} \quad (3)$$

n is the germinated seeds and D is the total number of days [42].

$$\text{Seed Vigor (SV)} = \text{GP} \times \text{Seedling length} \quad (4)$$

The emergence index was calculated as AOSA [43]:

$$\text{Emergence Index (EI)} = \frac{\text{Germinated seeds}}{\text{No of days of first count}} + \frac{\text{Germinated seeds}}{\text{No of days of final count}} \quad (5)$$

In addition, the time required for 50% emergence of seeds (E50) was calculated by Farooq et al. [44]:

$$E_{50} = t_i + \left[\left(N/2 - n_i \right) \left(t_j - t_i \right) \Big/ \left(n_j - n_i \right) \right] \quad (6)$$

where N is the final number of germinating seeds and n_j and n_i are the cumulative number of seeds germinated by the adjacent count at times t_j and t_i, respectively, when $n_i < N/2 < n_j$. According International Seed Testing Association (ISTA) lentils were used ten days after sowing for measurement of the different variables [45].

Preprints.org (www.preprints.org) | NOT PEER-REVIEWED | Posted: 8 July 2024 doi:10.20944/preprints202407.0589.v1

2.6. Statistical Analyses

Data analysis was performed using Infostat Software (InfoStat Group, Facultad de Ciencias Agropecuarias, Universidad Nacional de Córdoba, Argentina). The influence of the pyrolysis temperature on the characterization of BSG biochar was tested by one-way ANOVA (Section 3.2) and pyrolysis temperature and the dose of BSG biochar on germination test was tested by two-way ANOVA (Section 3.5) and Tukey's HSD test was used to found differences among media. All tests of significance were conducted at $p < 0.05$.

Response surface methodology was fitted using MATLAB R2015a software (The Mathworks Inc, Massachusetts, USA). The germination parameters such as GP, GR, MET, SV, EI, and E50 were predicted as a function of the dose of BSG biochar (%) and pyrolysis temperature (K). The goodness of fit and accuracy of the models were assessed and compared using statistical parameters such as the sum of squared errors (SSE), root-mean-squared error (RSME), and coefficient of determination (R^2) applying the formulas given in the Equations (7-9). The model giving the minimum values of SSE and RSME, but also presenting the highest R^2 was selected as the best model to express the corresponding responses.

$$SSE = \sum_{i=1}^{n} (y_p - y_e)^2 \quad (7)$$

$$RSME = \sqrt{\frac{1}{n} \sum_{i=1}^{n} (y_p - y_e)^2} \quad (8)$$

$$R^2 = 1 - \left(\sum_{i=1}^{n} (y_p - y_e)^2 / \sum_{i=1}^{n} (y_p - y_m)^2\right) \quad (9)$$

where y_p and y_e are the predicted and experimental data, respectively; y_m is the mean value of the experimental data, evaluated over a number n of experiments.

3. Results and Discussion

3.1. Bio-Waste Characterization

Table 1 shows the results of the proximate and ultimate analyses, pH, and EC of BSG. This biowaste had higher values of VM and lower values of ash, moisture, and FC than reported in the literature (Table 1). The results obtained for ash content were much lower than those reported by Zhang and Wang [46] and Sobek et al. [22], and similar values to those reported by Dudek et al. [47] and De Araújo et al. [26].

Table 1. Characteristics of BSG.

References	This study	Zhang and Wang [46]	Dudek et al. [47]	Yoo et al. [48]	Sobek et al. [22]	De Araújo et al. [26]
Moisture (%)	6.46 ± 0.05	-	-	-	7.52*	6.68 ± 0.58
VM (%)	90.01 ± 1.23	83.4 ± 2.8	-	-	73.15 ± 0.18	74.11 ± 0.42
FC (%)	7.71 ± 0.12	-	-	-	22.24 ± 0.24	16.44 ± 0.28
Ash (%)	2.27 ± 0.09	16.8 ± 0.8	3.10 ± 0.80	-	4.61 ± 0.22	2.78 ± 0.12
C (%)	46.09 ± 1.36	42.5 ± 2.5	50.47 ± 1.56	51.04 ± 1.37	52.66 ± 0.36	46.64*
O (%)	44.78 ± 2.16	-	34.37 ± 0.71	-	35.39 ± 0.33	39.62*
H (%)	5.88 ± 0.29	-	7.17 ± 0.06	-	7.66 ± 0.09	6.92*
N (%)	3.25 ± 0.05	3.7 ± 0.2	3.63 ± 0.09	3.96 ± 0.20	3.73 ± 0.12	3.84*
EC (μS/cm)	2912 ± 36	-	-	2690 ± 10	-	-
pH	5.49 ± 0.23	6.0 ± 0.1	-	5.20 ± 0.01	-	6.74*

Mean±SD; (*) values presented as mean only. Proximate analysis expressed on dry basis. VM (volatile matter); FC (fixed carbon); C (carbon content); O (oxygen content); H (hydrogen content); N (nitrogen content); EC (electrical conductivity).

Preprints.org (www.preprints.org) | NOT PEER-REVIEWED | Posted: 8 July 2024 doi:10.20944/preprints202407.0589.v1

It is important to note that, if ash content is less than 5–6%, the produced bio-oil does not exhibit knocking behavior [11]. As regards the ultimate analysis, the main components in BSG were C and O, while H and N were presented in minor proportions. Zhang and Wang [46] and De Araújo et al. [26] reported similar values of C and N content. Regarding the pH values, this was lower than those reported by Zhang and Wang [46] and De Araújo et al. [26] for BSG, while EC was lower than informed by Yoo et al. [48]. Differences presented could be due to barley variety, harvest time, geographic area, and conditions in the brewing process.

3.2. Yields and Properties of Obtained Biochars

Pyrolysis temperature influences the biochar properties. Biochar obtained at low temperatures is suitable for agricultural uses [49], while higher temperatures can improve particle porosity and thus improve its efficiency in adsorbing pollutants [50]. The biochar yield and physicochemical properties also vary with feedstock type, pyrolysis temperature, particle size, heating rate, residence time, operating pressure, and carrier gas flow rate [51–53]. The physicochemical properties of biochar determined were: ash content, pH, surface area, pore volume, and elemental composition such as C, H, N, O, and S [54,55]. The pyrolysis temperature (673, 773, and 873 K) significantly influenced the physicochemical properties of the BSG biochar (Table 2). The yield of BSG biochar decreased with increasing temperature due to the substantial release of volatile gases [56]. The yield of biochar obtained at 773 K was similar to that reported by Yinxin et al. [35]. The increase in pyrolysis temperature promotes a higher mass release, leading to biochar with higher ash and FC content. Consequently, due to the increase in FC content, biochar is more resistant to biological and thermal decomposition [56,57]. Similarly, Sánchez et al. [58] reported an increase in ash and FC contents of biochar compared to the original biomass and a decrease in moisture and VM contents.

The increase in ash content with pyrolysis temperature promotes the accumulation of inorganic mineral compounds, thereby enhancing the characteristics of BSG biochar for agricultural applications. To use biochar as an energy vector, low ash content is necessary due to the incrustation and corrosion problems [59]. The experimental biochar is composed primarily of C and O, followed by smaller proportions of N and H. Ultimate analysis of the samples revealed that C and N contents increased with the pyrolysis temperature, while O and H contents decreased with this variable. C content increased due to the carbonization process being more important, while O and H contents decreased as a consequence of the high pyrolysis temperature promoting the formation of aromatic compounds [60,61].

Table 2. Characteristics of the BSG biochar obtained at different pyrolysis temperatures.

Characteristics of the BSG biochar	Pyrolysis temperature (K)		
	673	773	873
Moisture (%)	4.66 ± 0.29^{a}	3.46 ± 0.26^{ab}	3.06 ± 0.11^{b}
VM (%)	52.83 ± 0.69^{a}	49.27 ± 2.02^{a}	29.21 ± 1.67^{b}
FC (%)	38.75 ± 2.00^{b}	42.14 ± 1.22^{b}	60.71 ± 3.18^{a}
Ash (%)	8.42 ± 0.65^{b}	8.59 ± 0.73^{b}	10.06 ± 0.24^{a}
C (%)	62.92 ± 2.11^{b}	64.51 ± 5.29^{b}	72.99 ± 4.88^{a}
O (%)	24.58 ± 0.35^{a}	22.93 ± 1.03^{a}	13.61 ± 0.25^{b}
H (%)	4.30 ± 0.14^{a}	4.09 ± 0.26^{a}	2.86 ± 0.11^{b}
N (%)	8.19 ± 0.29^{b}	8.46 ± 0.61^{b}	10.52 ± 0.93^{a}
H/C	0.82 ± 0.01^{a}	0.76 ± 0.04^{a}	0.47 ± 0.04^{a}
O/C	0.29 ± 0.01^{a}	0.27 ±0.02^{a}	0.14 ± 0.02^{a}
Yield (%)	38.04 ± 2.69^{a}	34.65 ± 1.94^{b}	31.52 ± 1.60^{c}
pH	7.15 ± 0.12^{a}	6.97 ± 0.33^{b}	6.73 ± 0.55^{b}

Preprints.org (www.preprints.org) | NOT PEER-REVIEWED | Posted: 8 July 2024 doi:10.20944/preprints202407.0589.v1

EC (μs/cm)	44.7 ± 3.07^{c}	72.8 ± 2.18^{a}	59.8 ± 2.99^{b}
WHC (%)	14.16 ± 0.60^{b}	15.32 ± 0.08^{a}	15.74 ± 0.65^{a}
Carbon retention (%)	51.93 ± 2.98^{ns}	48.50 ± 0.25^{ns}	49.92 ± 3.02^{ns}
Stable C mass fraction	0.344 ± 0.01^{c}	0.403 ± 0.01^{b}	0.687 ± 0.02^{a}
f_a	0.596 ± 0.02^{b}	0.632 ± 0.02^{b}	0.804 ± 0.05^{a}
R_{50}	0.117 ± 0.01^{ns}	0.120 ± 0.01^{ns}	0.138 ± 0.01^{ns}
CS	0.061 ± 0.01^{b}	0.058 ± 0.01^{b}	0.069 ± 0.01^{a}

Mean ± SD values followed by different superscripts within the same row are significantly different, with $p < 0.05$. "ns" denotes non-significance ($p \geq 0.05$). C (carbon content); O (oxygen content); H (hydrogen content); N (nitrogen content); EC (electrical conductivity); WHC (water holding capacity); f_a (aromaticity factor); R_{50} (recalcitrance potential); CS (carbon sequestration potential).

A significant decrease in the H/C and O/C atomic ratios was observed compared to the original bio-waste as pyrolysis temperature increased, evidencing a loss of oxygenated groups, a decrease of hydrophilicity and, an increase of carbonization degree and stability of biochar [11]. Consequently, the C-C bonds increased, and C-H and C-O bonds decreased due to dehydration, decarboxylation, and decarbonylation [59]. The N content increased from 8 to 10%. Similar results were obtained by Rodriguez-Ortiz et al. [11]. This aspect might be related to the recalcitrant nitrogen of the heterocyclic compounds in BSG and its carbonization [62]. In contrast, this result differs from that reported by Zhang and Wang [46] for the same biochar. The C/N ratios were 7.68, 7.62, and 6.93, for biochars obtained at 673, 773, and 873 K, respectively. With the increase of this ratio, the organic carbon of soil is strengthened, and the mineralization intensity of nitrogen decreases. The addition of biochar promotes the cation exchange capacity of the soil, adsorbing cations such as NH^{4+} and NO^{3-}, and decreases the N^2O release from the soil [63].

The pH values varied with the pyrolysis temperature, remaining around neutral pH, as the carbon forms carboxyl groups during the pyrolysis process, which lowers this parameter. This trend was not consistent with previous works [46,56]. According to pH values, the biochar obtained could be recommended for disposal in soils with an acidic, neutral, or slightly alkaline pH. It is important to note that biochar can be added to soil to buffer pH [64].

In addition, the EC values showed no clear trend concerning pyrolysis temperature, as was also observed by Rodriguez-Ortiz et al. [11] in nut and almond shells-based biochar. The obtained values indicated that a significant quantity of soluble salts was released.

For plant growth, WHC is very important because a high value of this parameter may improve water use in soilless cultivation [65]. Moreover, the WHC of BSG biochar increased with pyrolysis temperature due to the increased specific surface area. It is recognized that the stable C mass fraction present in the BSG biochar composition can increase soil stability due to its persistence. As expected, this characteristic increased with the pyrolysis temperature, although smoothly. The obtained R_{50} values increased with the temperature, and also, therefore, the stability of the BSG biochar. This parameter showed that the BSG biochar is similar to uncharred waste (intermediate stability) [11]. The CS of BSG biochar varies with the C aromaticity and interaction between organic C and mineral matter. When biochar is added to soil, its stability is improved as a consequence of the oxidation and formation of new mineral compounds or organic complexes. Considering the obtained results, it is observed that this parameter was highest at 873 K indicating high minerals covering the biochar surface [66].

As the majority of soil components, soil minerals enhance the stability of biochar towards oxidation by forming new minerals or organometallic complexes [67].

The highest retention value was observed for the BSG biochar obtained at 673 K; it can retain about 51.93% of the C content of BSG in the soil, with the consequent reduction of CO_2 release. Higher stable C mass fraction, carbon retention, R_{50}, and CS make BSG biochar a promising choice for carbon sequestration.

Preprints.org (www.preprints.org) | NOT PEER-REVIEWED | Posted: 8 July 2024 doi:10.20944/preprints202407.0589.v1

3.3. FTIR, EDS/SEM, and Specific Surface Area Analysis of BSG Biochar

The infrared spectra of the BSG biochar obtained at 673, 773, and 873 K are shown in Figure 2. The O-H-related peaks are located around 3500 1/cm, aliphatic C-H functional groups between 2900-2800 1/cm, and C=O functional groups between 1700-1600 1/cm. The presence of the 1200-1100 1/cm band revealed the presence of the C-O group, this peak increased at 873 K temperature. Peaks between 900 and 700 1/cm showed the presence of carboxylic acids and compounds with sulfur and/or halogens. The bands corresponding to 1588 and 1091 1/cm are typical of compounds with oxygenated and nitrogenous functional groups. The aliphatic groups tend to disappear with increasing temperature pyrolysis, this was observed by other authors in different biochars operating at different temperatures of the pyrolysis process [11,56].

It should be remarked that the peak intensity between 1700-1600 1/cm increased at 873 K, showing the formation of C=C bonds of a carbonaceous structure. At the same pyrolysis temperature, the peak intensity located around 3500 1/cm is intensified showing an increment of O-H bonds, confirming the obtained pH value.

The results of EDS analysis for the BSG biochar at 673, 773, and 873 K showed high C, Si, P, and K contents on the three examination surfaces (Figure 3). BSG biochar contained not only C, O, and Si, but also small amounts of different elements (Na, Mg, Ca, and K). These values were in agreement with Zhang and Wang [46], these authors reported similar values of Mg, Ca, and P contents.

Elements associated with the inorganic fraction of the BSG biochar could participate in the carbonization reaction and thus affect the pH, ash content, elemental composition, structure, and morphology of biochar [46]. It is observed that the intensity of the O peak decreased (decrease of O presence) with the pyrolysis temperature, which could be due to the high carbonization.

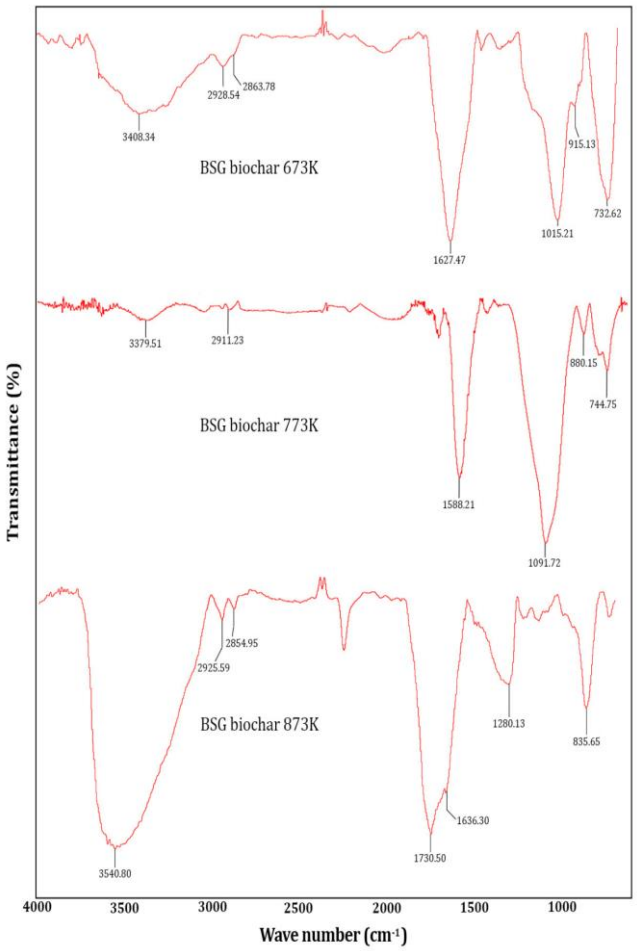

Figure 2. FTIR spectra of BSG biochar at 673 K, 773 K, and 873 K.

Preprints.org (www.preprints.org) | NOT PEER-REVIEWED | Posted: 8 July 2024 doi:10.20944/preprints202407.0589.v1

From Figure 4, the SEM images show that the carbonization promoted internal pores and cracks when BSG was pyrolyzed. This biochar presented an appreciable porous and tubular morphology. The average pore diameter of the BSG biochar increased with the pyrolysis temperature (8.88, 12.27, and 18.61 μm, at 673, 773, and 873 K respectively).

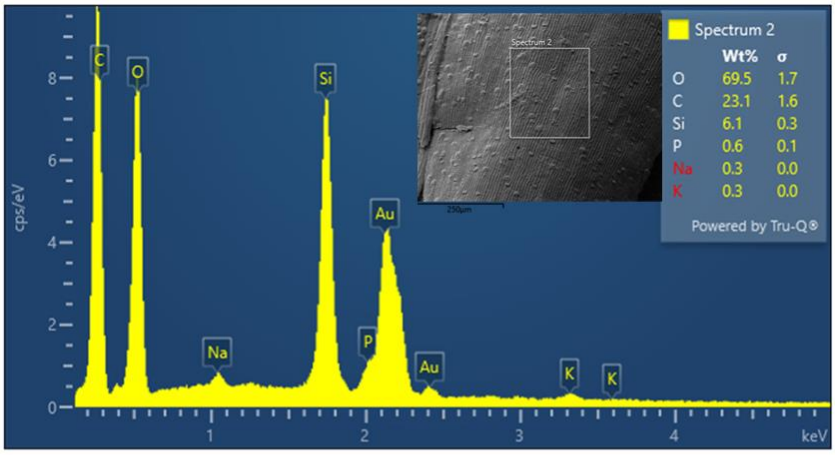

(a)

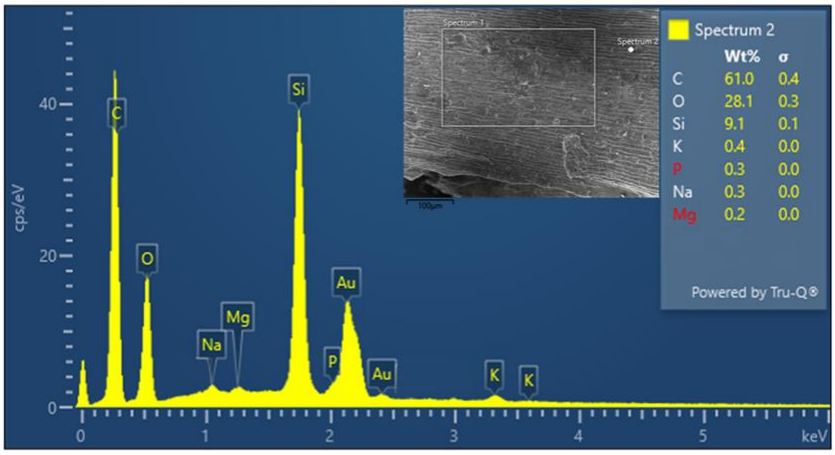

(b)

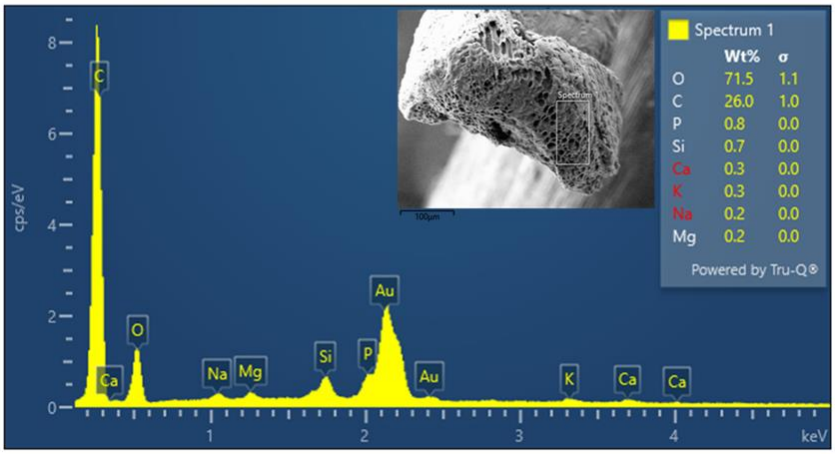

(c)

Figure 3. Results of the EDS test for BSG biochar at 673 K (**a**), 773 K (**b**), and 873 K (**c**). The Au peaks are a consequence of the gold bath carried out on the samples.

Preprints.org (www.preprints.org) | NOT PEER-REVIEWED | Posted: 8 July 2024 doi:10.20944/preprints202407.0589.v1

With the temperature increase, the BSG organic matter was gradually consumed, leading to an increase in the number of porous structures on the surface of the biochar [68].

The surface morphology of the BSG biochar was highly heterogeneous and structurally complex. Several authors concluded that structural changes in biochar particles were caused by variations in temperature, residence time, and gas circulation, leading to the deposition of condensed aromatic structures and biochar cracking [11,69,70]. The specific surface total areas, determined by the BET analysis corresponding to BSG biochar obtained at 673, 773, and 873 K were 3.50, 17.36, and 18.82 m^2/g, respectively. The highest surface area is observed at 873 K due to the highest gas release [11]. The specific surface area is a useful property to acknowledge the ability of soils to retain and transport nutrients and water [71]. In this sense, the incorporation of biochar in a soilless substrate would improve these aforementioned properties.

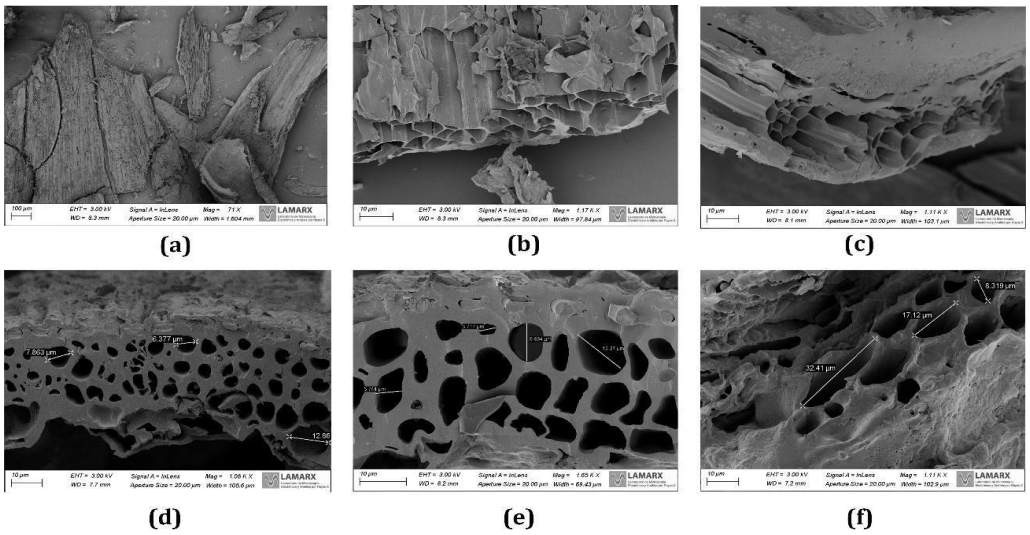

Figure 4. SEM images for biochar morphology at 673 K (a), 773 K (b), 873 K (c), and SEM images for the biochar porosity at 673 K (d), 773 K (e), 873 K (f).

3.4. Bioenergy Indices

Table 3 shows the bioenergy indices obtained for BSG and its biochar. For bioenergy production, a high BD value is a key property. The HHV was close to those reported by Dudek et al. [47] for the same waste type. The HHV values for BSG biochar ranged from 29.6 to 31.8 MJ/kg, according to the available reported experimental data [72].

Table 3. Bioenergy indices for the BSG and BSG biochar obtained at 673, 773, and 873 K.

Bioenergy indices	BSG	BSG biochar. Pyrolysis temperature (K)		
		673	773	873
HHV (MJ/kg)	18.63 ± 0.91^{c}	23.42 ± 1.45^{b}	23.90 ± 0.99^{ab}	26.43 ± 1.06^{a}
LHV (MJ/kg)	17.18 ± 1.02^{b}	22.35 ± 0.95^{ab}	22.91 ± 1.26^{ab}	25.72 ± 1.20^{a}
BD (GJ/m^3)	4.24 ± 0.22^{b}	5.30 ± 0.32^{a}	4.41 ± 0.28^{b}	4.27 ± 0.33^{b}
FVI[a]	1.99 ± 0.09^{a}	0.63 ± 0.04^{b}	0.51 ± 0.01^{bc}	0.42 ± 0.03^{c}
FFEV (petroleum)[b]	114.49 ± 6.48^{b}	143.19 ± 9.57^{a}	119.08 ± 8.22^{b}	115.21 ± 9.04^{b}
FFEV (diesel fuel)[b]	116.87 ± 9.62^{b}	146.17 ± 5.69^{a}	121.08 ± 6.81^{b}	117.61 ± 6.87^{b}
FFEV (fuel oil)[b]	106.16 ± 5.27^{b}	132.77 ± 3.26^{a}	110.41 ± 3.67^{b}	106.83 ± 7.58^{b}
FFEV (gasoline)[b]	129.97 ± 9.28^{b}	162.55 ± 12.88^{a}	135.18 ± 2.33^{b}	130.79 ± 8.56^{b}

Preprints.org (www.preprints.org) | NOT PEER-REVIEWED | Posted: 8 July 2024 doi:10.20944/preprints202407.0589.v1

PCOR (petroleum)[c]	392.70 ± 18.54[b]	491.15 ± 6.89[a]	408.44 ± 13.56[b]	395.18 ± 11.54[b]
PCOR (diesel fuel)[c]	412.55 ± 23.16[b]	515.98 ± 8.73[a]	429.09 ± 2.71[b]	415.15 ± 9.66[b]
PCOR (fuel oil)[c]	312.11 ± 9.12[b]	390.35 ± 2.34[a]	324.62 ± 9.38[b]	314.08 ± 13.29[b]
PCOR (gasoline)[c]	512.06 ± 10.04[b]	640.44 ± 9.96[a]	532.59 ± 9.66[ab]	515.29 ± 10.18[b]
E_d	-	1.26 ± 0.01[ns]	1.28 ± 0.11[ns]	1.42 ± 0.05[ns]
E_y (%)	-	47.82 ± 1.24[a]	44.45 ± 0.98[b]	44.72 ± 0.31[b]

[a] Usually expressed dimensionless; [b] [L fuel.m^3 biofuel]; [c] [kg CO_2.m^3 biofuel]. Means±SD. Different superscript letters in the same row indicate significant differences between groups (Tukey's HSD test, $p < 0.05$). "ns" denotes non-significance ($p \geq 0.05$). HHV (higher heat value); LHV (low heat value); BD (bioenergy density); FVI (fuel value index); FFEV (fossil fuel equivalent volume); PCOR (potential CO_2 retention); Ed (energy densification); Ey (energy yield).

It is observed that the HHV value of BSG biochar increased significantly with the pyrolysis temperature due to the carbonization process. Regarding the BSG biochar use as an energy vector, the HHV values were higher than those of raw BSG, evidencing the upgrading of this waste after the pyrolysis process. A similar trend was observed for the LHV values of BSG biochar. The obtained LHVs were comparable to those reported for coal reported by Sessa et al. [73].

The BD result of BSG was similar to those of its biochar obtained at pyrolysis temperatures of 773 and 873 K. Comparing the BD values for BSG and its biochar, it is observed that these biofuels have less capacity to generate energy than fossil fuels (37.03, 36.27, 39.93, and 32.62 GJ/m^3 for petroleum, diesel fuel, fuel oil, and gasoline, respectively). BSG presented a significantly higher FVI index than its biochar, primarily as a consequence of the higher ash content. Regarding FFEV and PCOR results, BSG biochar obtained at 673 K showed the best-performing biofuel. One cubic meter of this biochar generates bioenergy equivalent to 143.19, 146.17, 132.77, or 162.55 liters of petroleum, diesel fuel, fuel oil, and gasoline, respectively. Moreover, the use of this material as an energy vector can avoid the emission of up to 640 kg CO_2/m^3 biofuel, considering that it comes from lignocellulosic biomass which is a CO_2-neutral energy resource. From an environmental point of view, the use of any of these biofuels is advantageous, since they directly affect a reduction in the use of conventional non-renewable fuels.

The E_d values indicated that the HHV of BSG biochar was 26% to 42% higher compared to the HHV of raw BSG, although this increase was not statistically significant. This parameter increased with the pyrolysis temperature because H/C and O/C atomic ratios significantly decreased. E_y values of BSG biochar decreased with the pyrolysis temperature due to the decrease in yield associated with the mass loss caused by the carbonization reactions [59].

3.5. Germination and Growth of Lentil Seedlings

Figure 5 shows the photographs of the lentil germination assay in Petri dishes using four doses of BSG biochar at three different temperatures. In the soilless Petri dish trial, the pyrolysis temperature and its application dose significantly affected the germination of lentil seeds (Table 4, $p < 0.001$). In general, greater stability of the GR, EI, SV, and E_{50} variables was observed for the treatments with the BSG biochar obtained at 673 K.

Table 4. Effects of pyrolysis temperature (K) and dose (%) of biochar on germination parameters.

Dose (%)	GP (%)	GR	MET	SV	EI	E50
0	80.00 ± 2.30[b]	0.27 ± 0.01[c]	3.60 ± 0.16[ab]	284.45 ± 11.12[b]	10.10 ± 0.96[bcde]	1.50 ± 0.11[ab]
Pyrolysis temperature 673 K						
1	88.88 ± 2.98[e]	0.15 ± 0.01[b]	4.00 ± 0.23[bc]	329.13 ± 12.52[cd]	10.80 ± 0.81[de]	2.50 ± 0.26[d]
2	88.88 ± 5.11[e]	0.89 ± 0.04[f]	4.00 ± 0.23[bc]	319.01 ± 9.68[c]	11.80 ± 0.69[e]	2.50 ± 0.14[abc]

Preprints.org (www.preprints.org) | NOT PEER-REVIEWED | Posted: 8 July 2024 doi:10.20944/preprints202407.0589.v1

5	100.00 ± 6.03^{f}	0.04 ± 0.01^{a}	4.60 ± 0.18^{bc}	389.61 ± 7.25^{f}	8.30 ± 0.23^{ab}	4.67 ± 0.33^{d}
10	100.00 ± 3.15^{f}	0.06 ± 0.01^{ab}	4.60 ± 0.30^{bc}	448.96 ± 21^{h}	10.30 ± 0.87^{cde}	2.97 ± 0.17^{abcd}
Pyrolysis temperature 773 K						
1	84.44 ± 5.16^{d}	0.42 ± 0.01^{d}	3.80 ± 0.21^{ab}	344.25 ± 9.06^{b}	11.00 ± 0.56^{de}	2.88 ± 0.08^{abcd}
2	80.00 ± 2.05^{b}	0.08 ± 0.01^{ab}	3.60 ± 0.11^{ab}	262.98 ± 13.99^{a}	8.80 ± 0.18^{abc}	3.25 ± 0.09^{bcd}
5	100.00 ± 7.06^{f}	0.04 ± 0.01^{a}	5.80 ± 0.44^{c}	455.06 ± 16.87^{h}	8.10 ± 0.24^{a}	3.83 ± 0.15^{cd}
10	64.44 ± 4.18^{a}	0.64 ± 0.0^{3e}	1.90 ± 0.10^{a}	336.99 ± 6.74^{cd}	8.80 ± 0.30^{abc}	2.75 ± 0.12^{abcd}
Pyrolysis temperature 873 K						
1	84.44 ± 5.33^{d}	0.28 ± 0.01^{c}	3.80 ± 0.25^{ab}	320.38 ± 19.63^{c}	10.80 ± 0.63^{de}	1.58 ± 0.08^{ab}
2	100.00 ± 3^{f}	0.05 ± 0.01^{ab}	4.90 ± 0.26^{bc}	420.64 ± 8.77^{g}	9.90 ± 0.67^{abcde}	3.75 ± 0.13^{cd}
5	82.22 ± 6.24^{c}	0.09 ± 0.01^{ab}	3.70 ± 0.12^{ab}	364.84 ± 18.36^{e}	9.30 ± 0.55^{abcd}	1.94 ± 0.07^{abc}
10	80.00 ± 2.58^{b}	0.13 ± 0.01^{ab}	3.60 ± 0.19^{ab}	450.06 ± 15.18^{h}	9.60 ± 0.75^{abcd}	1.25 ± 0.11^{a}

Mean ± SD values followed by different superscripts within the same column are significantly different, with $p < 0.05$. GP (germination percentage); GR (germination rate); MET (mean emergence time); EI (emergence index); SV (seed vigor); E50 (time required for 50 % emergence of seeds).

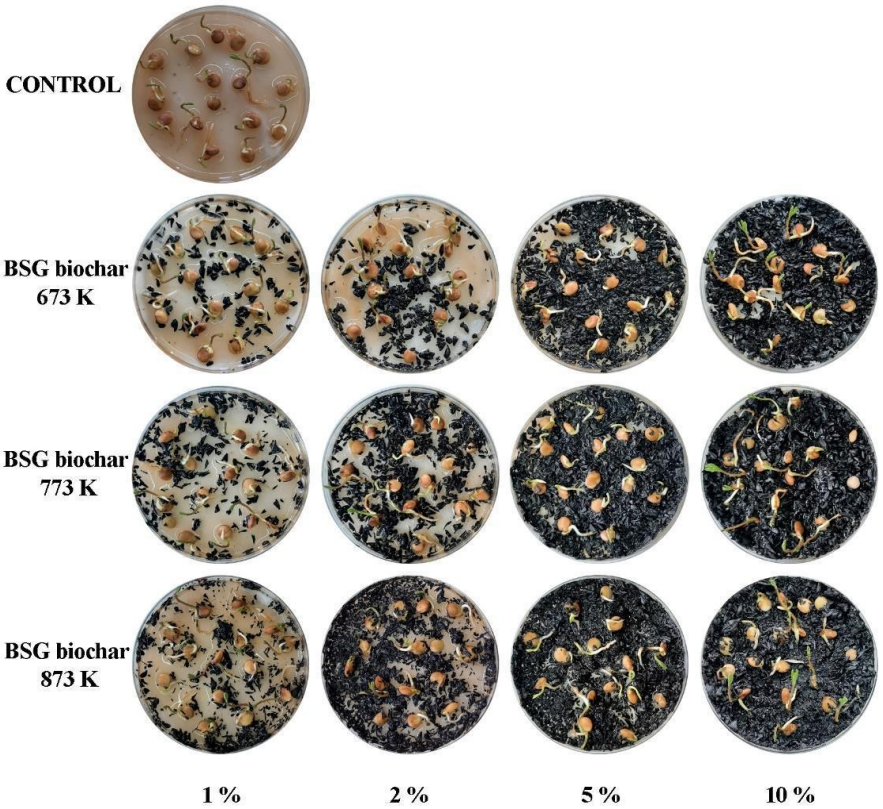

Figure 5. Photographs of germination assay of lentils in Petri dishes.

Germination of lentil seeds started on the fifth day, and the highest number of germinated seeds (total germinated seeds) was obtained when the doses of BSG biochar obtained at 673 K, 773 K, and 873 K, were 10%, 5%, and 2%, respectively. On the other hand, GR values were significant when the lentil seeds were germinated with doses equal to 2% and 10% of BSG biochar obtained at 673 K, and 773 K, respectively. The use of BSG biochar obtained at 873 K presented the lowest values of GR. A significant improvement in MET values was observed when the seeds were germinated with BSG biochar compared to the control. However, the lowest value of MET was found for the BSG biochar obtained at 773 K, added at 10%. Similarly, the results of SV demonstrated that lentil seedlings

Preprints.org (www.preprints.org) | NOT PEER-REVIEWED | Posted: 8 July 2024 doi:10.20944/preprints202407.0589.v1

growing in substrates with BSG biochar were longer than those in the control ones. Moreover, EI values were higher when the lentil seeds were germinated using the BSG biochar substrate with a dose of 2% (obtained at 673 K) and 1% (obtained at 773 and 873 K). The addition of BSG biochar had a positive influence on E50, except for the treatment with the highest rate of biochar (10%, obtained at 873 K). Ali et al. [39] reported that intermediate values of biochar ratios presented positive effects on seed germination and growth of corn seedlings. They worked with biochar obtained at 623 K and expressed that it improved the GR compared to the control treatment, while it caused a reduction in the MET value. The addition of biochar to sand at a ratio of 1.5% (w/w) significantly increased the dry biomass of the seedlings, the PG, and SV too, compared to the control treatment. Moreover, Solaiman et al. [40] demonstrated ratio-dependent negative effects of biochar on the germination and growth of wheat seedlings. This inhibition of seedling growth can be attributed to the reduced rate of cell division and cell elongation. Hafeez et al. [74] investigated the influence of corn cob biochar produced at 673 K on seed germination and seedling growth of soybean (*Glycine max* L. Merr.) under drought conditions, showing that when high ratios of biochar were applied (20 t/ha), SV, GP, and shoot length improved. The obtained results in this research are also consistent with those obtained by Ali et al. [39]. They evaluated the influence of biochar addition to the soil during corn seedling at a low rate (1.5% w/w), and reported an improvement in SV of 85%, while E50 did not show significative differences. Table 5 shows the fresh and dry weights of the harvested sprouts for each treatment.

Table 5. Effect of temperature and dose of biochar on lentil sprouts.

Treatment	Dose of biochar (%)	Fresh weight (g)	Dry weight (g)
Control	0	1.850 ± 0.042^{ns}	0.706 ± 0.058^{ns}
673 K	1	2.206 ± 0.102^{ns}	0.905 ± 0.034^{ns}
	2	2.136 ± 0.080^{ns}	0.975 ± 0.041^{ns}
	5	2.331 ± 0.031^{ns}	0.907 ± 0.028^{ns}
	10	1.918 ± 0.090^{ns}	0.760 ± 0.036^{ns}
773 K	1	2.182 ± 0.106^{ns}	0.924 ± 0.064^{ns}
	2	2.908 ± 0.062^{ns}	1.457 ± 0.088^{ns}
	5	1.800 ± 0.074^{ns}	0.837 ± 0.042^{ns}
	10	0.837 ± 0.012^{ns}	0.352 ± 0.024^{ns}
873 K	1	2.065 ± 0.121^{ns}	0.779 ± 0.051^{ns}
	2	2.087 ± 0.029^{ns}	0.858 ± 0.069^{ns}
	5	1.756 ± 0.016^{ns}	0.664 ± 0.043^{ns}
	10	1.987 ± 0.098^{ns}	0.757 ± 0.025^{ns}

Mean ± SD values followed by "ns" denote non-significance ($p \geq 0.05$).

In addition, it was determined that the temperature and the dose of biochar in Petri dishes did not significative influence lentils' weight. In contrast, Ali et al. [39] reported that at low doses (1.5% w/w) of corn cob biochar, maize seedlings recorded higher fresh weights than the control group, without biochar. Seed germination and emergence are essential for crop establishment. The positive effects of biochar on germination have been well documented in the literature [75–77]. The results revealed that in general, the addition of biochar improved germination parameters compared to the control. However, at the same pyrolysis temperature, the parameter values decreased with increasing doses of BSG biochar. Likewise, the pyrolysis temperature increase generated a decrease in these parameters. The causes of such best results adding BSG biochar could be related to the contents of 1) ash and 2) mineral elements, thus the biochar also contributed to their availability in the substrate, improving and accelerating the germination period, and finally 3) average internal pores present in

Preprints.org (www.preprints.org) | NOT PEER-REVIEWED | Posted: 8 July 2024 doi:10.20944/preprints202407.0589.v1

the BSG biochar, allowing water to fill the empty places, and maintaining the moisture in the Petri dishes. Based on the obtained results, it is suggested that BSG biochar could be employed as a component in soilless cultivation.

3.6. Variation of Germination Parameters with BSG Biochar Dose and Temperature

Table 6 shows the proposed models and their goodness of fit (x is pyrolysis temperature expressed in K and y is BSG biochar dose expressed in %). Most of the R^2 values were higher than 0.80, and SSE and RMSE parameters were low, indicating the good fit of the model to the experimental data. Hence, these models agree with the results obtained in this work. It is observed that GP and EI decreased with the BSG biochar dose and it is lowest at 773 K. At experimental conditions, GR is highest at the lowest BSG dose and pyrolysis temperature. MET showed the highest value at 873 K and 2% of the BSG biochar dose. On the other hand, SV is lowest at 773 K and increased with the BSG biochar dose. Finally, E_{50} increased with the pyrolysis temperature, and the BSG dose decreased. As can be seen, the BSG biochar obtained at 773 K presented the lowest indices, perhaps related to the P content on the surface. Figure 6 presents the parameters of germination assay under the studied conditions, using the response surface model.

Table 6. Goodness of fit by different models.

Model proposed	R^2	SSE	RMSE
GP (x,y) = 82.14 – 2.64·x – 2.873·y + 4.749·x^2 – 3.922·xy	0.8166	1.914	0.357
GR (x,y) = 0.3011 – 0.05094·x – 0.015274·y – 0.04769·x^2+ 0.05177·xy	0.9544	0.006	0.020
MET (x,y) = 3.875 – 0.07632·x – 0.3445·y + 0.1653·x^2 – 0.2232·xy	0.9336	0.257	0.1309
EI (x,y) = 9.396 – 0.1406·x – 0.5444·y + 0.3819·x^2 + 0.03734·xy	0.8583	1.299	0.2943
SV (x,y) = 346.6 + 6.117·x + 35.83·y + 18.31·x^2 – 6.459·xy	0.9812	0.575	0.619
E_{50} (x,y) = 3.139 – 0.6305·x – 0.2094·y – 0.1764·x^2 – 0.03753·xy	0.9488	0.4748	0.1779

GP (germination percentage); GR (germination rate); MET (mean emergence time); EI (emergence index); SV (seed vigor); E50 (time required for 50% emergence of seeds); x (pyrolysis temperature in fitting graphs); y (BSG biochar dose in fitting graphs); R^2 (coefficient of determination); SSE (sum of squared errors); RSME (root-mean-squared error).

Preprints.org (www.preprints.org) | NOT PEER-REVIEWED | Posted: 8 July 2024 doi:10.20944/preprints202407.0589.v1

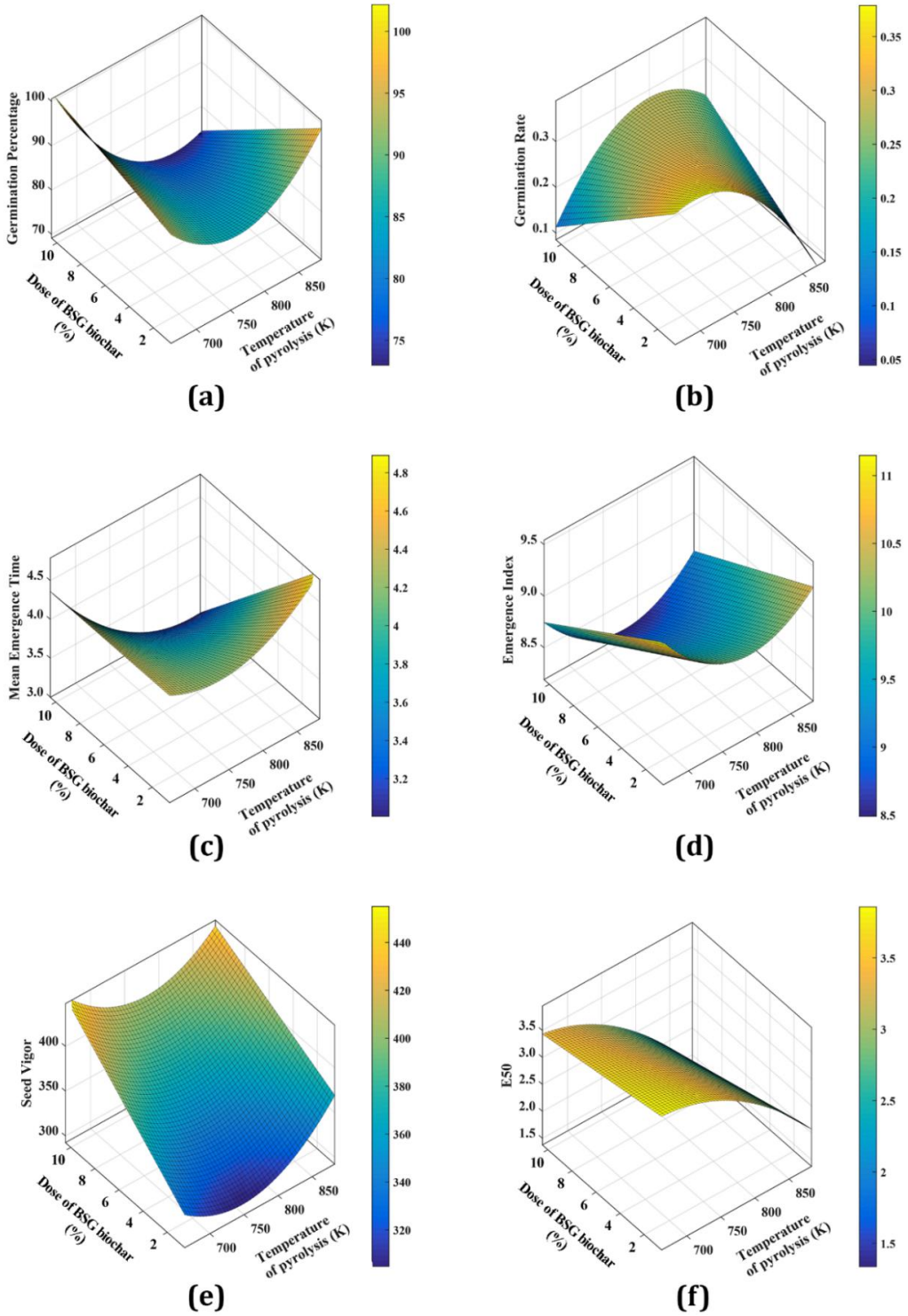

Figure 6. Effect of temperature of pyrolysis and dose of BSG biochar on GP (a), GR (b), MET (c), EI (d), SV (e), and E_{50} (f).

4. Conclusions

This research evaluates the potential use of BSG biochar as an energy vector and soilless constituent. The influence of the pyrolysis temperature on several main biochar physicochemical properties was investigated. All the BSG biochar obtained had high C content (> 62%) and low N content (< 10.52%), and an HHV higher than 23 MJ/kg, characteristics that indicate that the BSG biochar can be used as an energy vector. Considering the pyrolysis temperature effect, E_d increased

Preprints.org (www.preprints.org) | NOT PEER-REVIEWED | Posted: 8 July 2024 doi:10.20944/preprints202407.0589.v1

with this parameter showing that the HHV of BSG biochar was higher than that of raw BSG, however, E_y decreased due to a drop in the yield of BSG biochar.

On the other hand, the pH values of BSG biochar obtained at all pyrolysis temperatures were about 7. Therefore, the BSG biochar can be added to neutral or slightly alkaline soil to buffer pH. WHC, R_{50}, and CS increased with the temperature pyrolysis showed that the BSG biochar obtained at 873 K is the most stable biochar and should improve the water use in soilless cultivation. The highest carbon retention was found for the BSG biochar obtained at 673 K, indicating the lowest CO_2 release. Consequently, BSG biochar is a promising choice for carbon sequestration due to the values of stable C mass fraction, carbon retention, R_{50}, and CS. The surface morphology of the BSG biochar was highly heterogeneous and structurally complex and the specific surface total area increased with the pyrolysis temperature. Moreover, BSG biochar contains small amounts of different elements such as Na, Mg, Ca, and K.

Based on BD, FVI, FFEV, and PCOR evaluations, biochar obtained at 673 K is optimal as an energy vector. It provides more energy per unit volume than biochar obtained at 773 and 873 K, with lower ash content, thereby enhancing its fuel efficiency, flammability, and heat generation characteristics. Compared to fossil fuels, it exhibits greater potential for CO_2 retention, contributing to its environmental sustainability as a renewable energy source.

From the germination test, the possible use of BSG biochar added at different doses as a constituent substrate is highlighted. The variables GP, MET, and SV showed good results when BSG biochar obtained at 773 K was applied at a dose of 5% w/w.

During the pyrolysis process, not only is biochar obtained, but also gas and bio-oil. Depending on their characteristics, these byproducts can be used as energy vectors or as raw materials for various processes to produce other value-added products. This process can be employed in countryside areas, promoting the development of companies that will obtain energy vectors and substrate for soilless cultivation and offer solutions for generated BSG management, with a high and positive social, economic, and environmental impact. The sustainable valorization of BSG through pyrolysis not only diverts waste from landfills but also contributes to renewable energy production and sustainable agricultural practices. By transforming industrial by-products into valuable resources, this approach aligns with global sustainability goals and fosters environmental stewardship. Additionally, the process supports rural development by creating opportunities for local enterprises and enhancing resource efficiency.

Supplementary Materials: The following supporting information can be downloaded at: Preprints.prg, A: Equations for BSG biochar characterization and B: Equations used in Bioenergy Indices

Author Contributions: Romina Zabaleta: Conceptualization, Formal analysis, Investigation, Writing - original draft; Software. Erick Torres: Formal analysis, Validation, Writing - original draft; Software. Eliana Sánchez Methodology, Investigation, Writing - original draft. Rodrigo Torres-Sciancalepore: Formal analysis, Writing - original draft. María Paula Fabani: Conceptualization, Methodology, Investigation, Funding acquisition. Germán Mazza: Visualization, Resources, Writing - review & editing, Project administration, Funding acquisition. Rosa Rodriguez: Resources, Writing - review & editing, Supervision, Project administration, Funding acquisition.

Funding: The authors wish to thank the support of the following Argentine institutions: the University of San Juan (PDTS Res. 1054/18) (PROJOVI Resol. 1500/23-R); the University of Comahue (PIN 2022-04/I260); National Scientific and Technical Research Council, CONICET (Project PUE PROBIEN-CONICET 22920150100067 and PIP 2021-2023 – No. 11220200100950CO); FONCYT-PICT RESOL-2023-31-APN-DANPIDTYI#ANPID TYI (PICT-2021-A-0067). FONCYT-PICTA RESOL-2022-87 Project Number 20 (2022). Romina Zabaleta, Erick Torres, Eliana Sánchez, and Rodrigo Torres-Sciancalepore have doctoral fellowships from CONICET. Maria Paula Fabani, Rosa Rodriguez and Germán Mazza are Research Members of CONICET, Argentina.

Informed Consent Statement: Not applicable.

Data Availability Statement: The datasets generated during the current study are available from the corresponding author upon reasonable request.

Preprints.org (www.preprints.org) | NOT PEER-REVIEWED | Posted: 8 July 2024 doi:10.20944/preprints202407.0589.v1

Acknowledgments: The authors would like to express their gratitude to the "Cumbre" brewery, located in San Juan Province, Argentina for providing the brewer's spent grain.

Conflicts of Interest: The authors declare no conflicts of interest

Nomenclature

EC	Electrical conductivity, (µS/cm)
BD	Bioenergy density, (GJ/m^3)
BSG	Brewer´s spent grain
C	Carbon content, (%)
CS	Carbon sequestration potential, (dimensionless)
D	Total number of days
E50	Time required for 50 % emergence of seeds
EC	Electrical conductivity, (µS/cm)
E_d	Energy densification, (dimensionless)
EDS	Energy dispersive X-ray spectroscopy
EI	Emergence index, (dimensionless)
E_y	Energy yield, (%)
f_a	Aromaticity factor, (dimensionless)
FC	Fixed carbon content, (%)
FFEV	Fossil fuel equivalent volume, (L fuel/ m^3 biofuel)
FTIR	Fourier transform infrared
FVI	Fuel value index, (dimensionless)
g	Total number of germinated seeds
GP	Germination percentage, (%)
GR	Germination rate
H	Hydrogen content, (%)
HHV	Higher heat value, (MJ/kg)
LHV	Low heat value, (MJ/kg)
MET	Mean emergence time
MRT	Response surface methodology
N	Final number of germinating seeds
n	Germinated seed
n	Number of experiments
N	Number of germinated seeds
N	Nitrogen content, (%)
n	Seeds germinated on growth day
n_i	Number of seeds germinated count at time ti
n_j	Number of seeds germinated count at time tj
PCOR	Potential CO_2 retention, (kg CO_2/ m^3 biofuel)
R^2	Coefficient of determination
R_{50}	Recalcitrance potential, (dimensionless)

Preprints.org (www.preprints.org) | NOT PEER-REVIEWED | Posted: 8 July 2024 doi:10.20944/preprints202407.0589.v1

RSME Root-mean-squared error

S Sulfur content, (%)

SD Standard deviation

SEM Scanning Electron Microscopy

SN0 Total number of viable seeds

SNG Germinated seed in total

SSE Sum of squared errors

SV Seed vigor, (%)

VM Volatile matter, (%)

WHC Water holding capacity, (%)

x Pyrolysis temperature in fitting graphs, (K)

y BSG biochar dose in fitting graphs, (%)

y_e Experimental data

y_m Mean value of the experimental data

y_p Predicted data

z Response variables in fitting graphs

References

1. Carlini, M.; Monarca, D.; Castellucci, S.; Mennuni, A.; Casini, L.; Selli, S. Beer Spent Grains Biomass for Biogas Production: Characterization and Anaerobic Digestion-Oriented Pre-Treatments. Energy Reports 2021, 7, 921–929, doi:10.1016/j.egyr.2021.07.049.
2. Franciski, M.A.; Peres, E.C.; Godinho, M.; Perondi, D.; Foletto, E.L.; Collazzo, G.C.; Dotto, G.L. Development of CO_2 Activated Biochar from Solid Wastes of a Beer Industry and Its Application for Methylene Blue Adsorption. Waste Manag. 2018, 78, 630–638, doi:10.1016/j.wasman.2018.06.040.
3. FAO. Production Quantities of Beer by Country. Food and Agriculture Organization of the United Nations. FAOSTAT, Food and Agriculture Data.
4. Gonçalves, G. da C.; Nakamura, P.K.; Furtado, D.F.; Veit, M.T. Utilization of Brewery Residues to Produces Granular Activated Carbon and Bio-Oil. J. Clean. Prod. 2017, 168, 908–916, doi:10.1016/j.jclepro.2017.09.089.
5. Ikram, S.; Huang, L.Y.; Zhang, H.; Wang, J.; Yin, M. Composition and Nutrient Value Proposition of Brewers Spent Grain. J. Food Sci. 2017, 82, 2232–2242, doi:10.1111/1750-3841.13794.
6. Mussatto, S.I. Brewer's Spent Grain: A Valuable Feedstock for Industrial Applications. J. Sci. Food Agric. 2014, 94, 1264–1275, doi:10.1002/jsfa.6486.
7. Saraiva, B.R.; Agustinho, B.C.; Vital, A.C.P.; Staub, L.; Matumoto Pintro, P.T. Effect of Brewing Waste (Malt Bagasse) Addition on the Physicochemical Properties of Hamburgers. J. Food Process. Preserv. 2019, 43, 1–9, doi:10.1111/jfpp.14135.
8. Faccenda, A.; Zambom, M.A.; de Avila, A.S.; Schneider, C.R.; Werle, C.H.; Anschau, F.A.; Almeida, A.R.E.; Lange, M.J.; dos Santos, G.T. Performance and Milk Composition of Holstein Cows Fed with Dried Malt Bagasse and Selenium-Enriched Saccharomyces Cerevisiae. Livest. Sci. 2020, 238, 104081, doi:10.1016/j.livsci.2020.104081.
9. Buller, L.S.; Sganzerla, W.G.; Lima, M.N.; Muenchow, K.E.; Timko, M.T.; Forster-Carneiro, T. Ultrasonic Pretreatment of Brewers' Spent Grains for Anaerobic Digestion: Biogas Production for a Sustainable Industrial Development. J. Clean. Prod. 2022, 355, doi:10.1016/j.jclepro.2022.131802.
10. Fernandez, A.; Sette, P.; Echegaray, M.; Soria, J.; Salvatori, D.; Mazza, G.; Rodriguez, R. Clean Recovery of Phenolic Compounds, Pyro-Gasification Thermokinetics, and Bioenergy Potential of Spent Agro-Industrial Bio-Wastes. Biomass Convers. Biorefinery 2022, doi:10.1007/s13399-021-02197-z.
11. Rodriguez Ortiz, L.; Torres, E.; Zalazar, D.; Zhang, H.; Rodriguez, R.; Mazza, G. Influence of Pyrolysis Temperature and Bio-Waste Composition on Biochar Characteristics. Renew. Energy 2020, 155, 837–847, doi:10.1016/j.renene.2020.03.181.
12. Zalazar-Garcia, D.; Fernandez, A.; Cavaliere, L.; Deng, Y.; Soria, J.; Rodriguez, R.; Mazza, G. Slow Pyrolysis of Pistachio-Waste Pellets: Combined Phenomenological Modeling with Environmental, Exergetic, and Energetic Analysis (3-E). Biomass Convers. Biorefinery 2022, doi:10.1007/s13399-022-03232-3.
13. Zeng, K.; Gauthier, D.; Lu, J.; Flamant, G. Parametric Study and Process Optimization for Solar Pyrolysis of Beech Wood. Energy Convers. Manag. 2015, 106, 987–998, doi:10.1016/j.enconman.2015.10.039.

Preprints.org (www.preprints.org) | NOT PEER-REVIEWED | Posted: 8 July 2024 doi:10.20944/preprints202407.0589.v1

14. Soria, J.; Li, R.; Flamant, G.; Mazza, G.D. Influence of Pellet Size on Product Yields and Syngas Composition during Solar-Driven High Temperature Fast Pyrolysis of Biomass. J. Anal. Appl. Pyrolysis 2019, 140, 299–311, doi:10.1016/j.jaap.2019.04.007.
15. Liang, Q.; Pan, D.; Zhang, X. Construction and Application of Biochar-Based Composite Phase Change Materials. Chem. Eng. J. 2023, 453, 139441, doi:10.1016/j.cej.2022.139441.
16. Ganesapillai, M.; Mehta, R.; Tiwari, A.; Sinha, A.; Bakshi, H.S.; Chellappa, V.; Drewnowski, J. Waste to Energy: A Review of Biochar Production with Emphasis on Mathematical Modelling and Its Applications. Heliyon 2023, 9, e14873, doi:10.1016/j.heliyon.2023.e14873.
17. Protásio, T. de P.; Bufalino, L.; Tonoli, G.H.D.; Guimarães Junior, M.G.; Trugilho, P.F.; Mendes, L.M. Brazilian Lignocellulosic Wastes for Bioenergy Production: Characterization and Comparison with Fossil Fuels. BioResources 2013, 8, 1166–1185, doi:10.15376/biores.8.1.1166-1185.
18. Zabaleta, R.; Sánchez, E.; Fabani, P.; Mazza, G.; Rodriguez, R. Almond Shell Biochar: Characterization and Application in Soilless Cultivation of Eruca Sativa. Biomass Convers. Biorefinery 2023, doi:10.1007/s13399-023-04002-5.
19. Mir, S.A.; Farooq, S.; Shah, M.A.; Sofi, S.A.; Dar, B.N.; Hamdani, A.M.; Mousavi Khaneghah, A. An Overview of Sprouts Nutritional Properties, Pathogens and Decontamination Technologies. Lwt 2021, 141, 110900, doi:10.1016/j.lwt.2021.110900.
20. Liu, H.K.; Li, Z.H.; Zhang, X.W.; Liu, Y.P.; Hu, J.G.; Yang, C.W.; Zhao, X.Y. The Effects of Ultrasound on the Growth, Nutritional Quality and Microbiological Quality of Sprouts. Trends Food Sci. Technol. 2021, 111, 292–300, doi:10.1016/j.tifs.2021.02.065.
21. Dessì, F.; Mureddu, M.; Ferrara, F.; Pettinau, A. A Comprehensive Pathway on the Determination of the Kinetic Triplet and the Reaction Mechanism of Brewer's Spent Grain and Beech Wood Chips Pyrolysis. Renew. Energy 2022, 190, 548–559, doi:10.1016/j.renene.2022.03.084.
22. Sobek, S.; Zeng, K.; Werle, S.; Junga, R.; Sajdak, M. Brewer's Spent Grain Pyrolysis Kinetics and Evolved Gas Analysis for the Sustainable Phenolic Compounds and Fatty Acids Recovery Potential. Renew. Energy 2022, 199, 157–168, doi:10.1016/j.renene.2022.08.114.
23. Ashman, C.H.; Gao, L.; Goldfarb, J.L. Silver Nitrate in Situ Upgrades Pyrolysis Biofuels from Brewer's Spent Grain via Biotemplating. J. Anal. Appl. Pyrolysis 2020, 146, 104729, doi:10.1016/j.jaap.2019.104729.
24. Emmanuel, J.K.; Nganyira, P.D.; Shao, G.N. Evaluating the Potential Applications of Brewers' Spent Grain in Biogas Generation, Food and Biotechnology Industry: A Review. Heliyon 2022, 8, e11140, doi:10.1016/j.heliyon.2022.e11140.
25. Olszewski, M.P.; Arauzo, P.J.; Wądrzyk, M.; Kruse, A. Py-GC-MS of Hydrochars Produced from Brewer's Spent Grains. J. Anal. Appl. Pyrolysis 2019, 140, 255–263, doi:10.1016/j.jaap.2019.04.002.
26. de Araújo, T.P.; Quesada, H.B.; Bergamasco, R.; Vareschini, D.T.; de Barros, M.A.S.D. Activated Hydrochar Produced from Brewer's Spent Grain and Its Application in the Removal of Acetaminophen. Bioresour. Technol. 2020, 310, 123399, doi:10.1016/j.biortech.2020.123399.
27. Maqhuzu, A.B.; Yoshikawa, K.; Takahashi, F. Prospective Utilization of Brewers' Spent Grains (BSG) for Energy and Food in Africa and Its Global Warming Potential. Sustain. Prod. Consum. 2021, 26, 146–159, doi:10.1016/j.spc.2020.09.022.
28. Capossio, J.P.; Fabani, M.P.; Reyes-Urrutia, A.; Torres-Sciancalepore, R.; Deng, Y.; Baeyens, J.; Rodriguez, R.; Mazza, G. Sustainable Solar Drying of Brewer's Spent Grains: A Comparison with Conventional Electric Convective Drying. Processes 2022, 10, 1–18, doi:10.3390/pr10020339.
29. ASTM E872 - 82 Standard Test Method for Volatile Matter in the Analysis of Particulate Wood Fuels. ASTM Int. 1998, 14-16. Accessed date: October 2019.
30. ASTM D 1102–84 Standard Test Method for Ash in Wood1 2001, 2. Accessed date: September 2019.
31. Lorente, A.; Remón, J.; Salgado, M.; Huertas-Alonso, A.J.; Sánchez-Verdú, P.; Moreno, A.; Clark, J.H. Sustainable Production of Solid Biofuels and Biomaterials by Microwave-Assisted, Hydrothermal Carbonization (MA-HTC) of Brewers' Spent Grain (BSG). ACS Sustain. Chem. Eng. 2020, 8, 18982–18991.
32. ASTM E873-82. Standard Test Method for Bulk Density of Densified Particulate Biomass Fuels–ASTM International. West Conshohocken, PA, USA 2013.
33. Bu, X.; Ji, H.; Ma, W.; Mu, C.; Xian, T.; Zhou, Z.; Wang, F.; Xue, J. Effects of Biochar as a Peat-Based Substrate Component on Morphological, Photosynthetic and Biochemical Characteristics of Rhododendron Delavayi Franch. Sci. Hortic. (Amsterdam). 2022, 302, 111148, doi:10.1016/j.scienta.2022.111148.
34. Chun, Y.; Sheng, G.; Chiou, G.T.; Xing, B. Compositions and Sorptive Properties of Crop Residue-Derived Chars. Environ. Sci. Technol. 2004, 38, 4649–4655, doi:10.1021/es035034w.
35. Yinxin, Z.; Jishi, Z.; Yi, M. Preparation and Application of Biochar from Brewery`s Spent Grain and Sewage Sludge. Open Chem. Eng. J. 2015, 9, 14–19, doi:10.2174/1874123101509010014.
36. Torres-Sciancalepore, R.; Fernandez, A.; Asensio, D.; Riveros, M.; Fabani, M.P.; Fouga, G.; Rodriguez, R.; Mazza, G. Kinetic and Thermodynamic Comparative Study of Quince Bio-Waste Slow Pyrolysis before and after Sustainable Recovery of Pectin Compounds. Energy Convers. Manag. 2022, 252, 115076, doi:10.1016/j.enconman.2021.115076.

Preprints.org (www.preprints.org) | NOT PEER-REVIEWED | Posted: 8 July 2024 doi:10.20944/preprints202407.0589.v1

37. Alves, J.L.F.; da Silva, J.C.G.; Mumbach, G.D.; Domenico, M. Di; da Silva Filho, V.F.; de Sena, R.F.; Machado, R.A.F.; Marangoni, C. Insights into the Bioenergy Potential of Jackfruit Wastes Considering Their Physicochemical Properties, Bioenergy Indicators, Combustion Behaviors, and Emission Characteristics. Renew. Energy 2020, 155, 1328–1338, doi:10.1016/j.renene.2020.04.025.
38. Contreras, M. del M.; Lama-Muñoz, A.; Romero-García, J.M.; García-Vargas, M.; Romero, I.; Castro, E. Production of Renewable Products from Brewery Spent Grains. Waste Biorefinery 2021, 305–347, doi:10.1016/B978-0-12-821879-2.00011-9.
39. Ali, L.; Xiukang, W.; Naveed, M.; Ashraf, S.; Nadeem, S.M.; Haider, F.U.; Mustafa, A. Impact of Biochar Application on Germination Behavior and Early Growth of Maize Seedlings: Insights from a Growth Room Experiment. Appl. Sci. 2021, 11, 1–13, doi:10.3390/app112411666.
40. Solaiman, Z.M.; Murphy, D. V.; Abbott, L.K. Biochars Influence Seed Germination and Early Growth of Seedlings. Plant Soil 2012, 353, 273–287, doi:10.1007/s11104-011-1031-4.
41. Scott, S.J.; Jones, R.A.; Williams, W.. Review of Data Analysis Methods for Seed Germination. Crop Sci 1984, 24, 1192–1199, doi:https://doi.org/10.2135/cropsci1984.0011183X002400060043x.
42. Ellis, R.A.; Roberts, E. The Quantification of Ageing and Survival in Orthodox Seeds. Seed Sci. Technol. 1981, 9, 373–409.
43. AOSA. Rules for Testing Seeds. In Journal of Seed Technology; 1990; pp. 1–112.
44. Farooq, M.; Basra, S.M.A.; Ahmad, N.; Hafeez, K. Thermal Hardening: A New Seed Vigor Enhancement Tool in Rice. J. Integr. Plant Biol. 2005, 47, 187–193, doi:10.1111/j.1744-7909.2005.00031.x.
45. ISTA Reglas Internacionales Para El Analisis de Las Semillas. Int. Rules Seed Test. 2016, 192.
46. Zhang, J.; Wang, Q. Sustainable Mechanisms of Biochar Derived from Brewers' Spent Grain and Sewage Sludge for Ammonia-Nitrogen Capture. J. Clean. Prod. 2016, 112, 3927–3934, doi:10.1016/j.jclepro.2015.07.096.
47. Dudek, M.; Świechowski, K.; Manczarski, P.; Koziel, J.A.; Białowiec, A. The Effect of Biochar Addition on the Biogas Production Kinetics from the Anaerobic Digestion of Brewers' Spent Grain. Energies 2019, 12, 1–22, doi:10.3390/en12081518.
48. Yoo, J.H.; Luyima, D.; Lee, J.H.; Park, S.Y.; Yang, J.W.; An, J.Y.; Yun, Y.U.; Oh, T.K. Effects of Brewer's Spent Grain Biochar on the Growth and Quality of Leaf Lettuce (Lactuca Sativa L. Var. Crispa.). Appl. Biol. Chem. 2021, 64, doi:10.1186/s13765-020-00577-z.
49. Sanchez, E.; Zabaleta, R.; Navas, A.L.; Torres-Sciancalepore, R.; Fouga, G.; Fabani, M.P.; Rodriguez, R.; Mazza, G. Assessment of Pistachio Shell-Based Biochar Application in the Sustainable Amendment of Soil and Its Performance in Enhancing Bell Pepper (Capsicum Annuum L.) Growth. Sustainability 2024, 16, 4429, doi:https://doi.org/10.3390/su16114429.
50. Agrafioti, E.; Bouras, G.; Kalderis, D.; Diamadopoulos, E. Biochar Production by Sewage Sludge Pyrolysis. J. Anal. Appl. Pyrolysis 2013, 101, 72–78, doi:10.1016/j.jaap.2013.02.010.
51. Asensio, V.; Vega, F.A.; Andrade, M.L.; Covelo, E.F. Tree Vegetation and Waste Amendments to Improve the Physical Condition of Copper Mine Soils. Chemosphere 2013, 90, 603–610, doi:10.1016/J.CHEMOSPHERE.2012.08.050.
52. Yinxin Z, Jishi Z, Y.M. Preparation and Application of Biochar from Brewery`s Spent Grain and Sewage Sludge. Open Chem. Eng. J. 2015, 9: 14–19, doi:https://doi.org/10.2174/1874123101509010014.
53. Tripathi, M.; Sahu, J.N.; Ganesan, P. Effect of Process Parameters on Production of Biochar from Biomass Waste through Pyrolysis: A Review. Renew. Sustain. Energy Rev. 2016, 55, 467–481, doi:10.1016/J.RSER.2015.10.122.
54. Kambo, H.S.; Dutta, A. A Comparative Review of Biochar and Hydrochar in Terms of Production, Physico-Chemical Properties and Applications. Renew. Sustain. Energy Rev. 2015, 45, 359–378, doi:10.1016/J.RSER.2015.01.050.
55. Liu, N.; Charrua, A.B.; Weng, C.H.; Yuan, X.; Ding, F. Characterization of Biochars Derived from Agriculture Wastes and Their Adsorptive Removal of Atrazine from Aqueous Solution: A Comparative Study. Bioresour. Technol. 2015, 198, 55–62, doi:10.1016/J.BIORTECH.2015.08.129.
56. Rafiq, M.K.; Bachmann, R.T.; Rafiq, M.T.; Shang, Z.; Joseph, S.; Long, R.L. Influence of Pyrolysis Temperature on Physico-Chemical Properties of Corn Stover (Zea Mays l.) Biochar and Feasibility for Carbon Capture and Energy Balance. PLoS One 2016, 11, 1–17, doi:10.1371/journal.pone.0156894.
57. Campos, P.; Miller, A.Z.; Knicker, H.; Costa-Pereira, M.F.; Merino, A.; De la Rosa, J.M. Chemical, Physical and Morphological Properties of Biochars Produced from Agricultural Residues: Implications for Their Use as Soil Amendment. Waste Manag. 2020, 105, 256–267, doi:10.1016/j.wasman.2020.02.013.
58. Sánchez, E.; Zabaleta, R.; Fabani, M.P.; Rodriguez, R.; Mazza, G. Effects of the Amendment with Almond Shell, Bio-Waste and Almond Shell-Based Biochar on the Quality of Saline-Alkali Soils. J. Environ. Manage. 2022, 318, doi:10.1016/j.jenvman.2022.115604.
59. de Almeida, S.G.C.; Tarelho, L.A.C.; Hauschild, T.; Costa, M.A.M.; Dussán, K.J. Biochar Production from Sugarcane Biomass Using Slow Pyrolysis: Characterization of the Solid Fraction. Chem. Eng. Process. - Process Intensif. 2022, 179, doi:10.1016/j.cep.2022.109054.

Preprints.org (www.preprints.org) | NOT PEER-REVIEWED | Posted: 8 July 2024 doi:10.20944/preprints202407.0589.v1

60. Abbas, Q.; Liu, G.; Yousaf, B.; Ali, M.U.; Ullah, H.; Munir, M.A.M.; Liu, R. Contrasting Effects of Operating Conditions and Biomass Particle Size on Bulk Characteristics and Surface Chemistry of Rice Husk Derived-Biochars. J. Anal. Appl. Pyrolysis 2018, 134, 281–292, doi:10.1016/j.jaap.2018.06.018.
61. Tomczyk, A.; Sokołowska, Z.; Boguta, P. Biochar Physicochemical Properties: Pyrolysis Temperature and Feedstock Kind Effects. Rev. Environ. Sci. Biotechnol. 2020, 19, 191–215, doi:10.1007/s11157-020-09523-3.
62. Almendros, G.; Knicker, H.; González-Vila, F.J. Rearrangement of Carbon and Nitrogen Forms in Peat after Progressive Thermal Oxidation as Determined by Solid-State 13C- and 15N-NMR Spectroscopy. Org. Geochem. 2003, 34, 1559–1568, doi:10.1016/S0146-6380(03)00152-9.
63. Xu, H.; Cai, A.; Wu, D.; Liang, G.; Xiao, J.; Xu, M.; Colinet, G.; Zhang, W. Effects of Biochar Application on Crop Productivity, Soil Carbon Sequestration, and Global Warming Potential Controlled by Biochar C: N Ratio and Soil PH: A Global Meta-Analysis. Soil Tillage Res. 2021, 213, doi:10.1016/j.still.2021.105125.
64. Fatima, B.; Bibi, F.; Ishtiaq Ali, M.; Woods, J.; Ahmad, M.; Mubashir, M.; Shariq Khan, M.; Bokhari, A.; Khoo, K.S. Accompanying Effects of Sewage Sludge and Pine Needle Biochar with Selected Organic Additives on the Soil and Plant Variables. Waste Manag. 2022, 153, 197–208, doi:10.1016/j.wasman.2022.08.016.
65. Lataf, A.; Jozefczak, M.; Vandecasteele, B.; Viaene, J.; Schreurs, S.; Carleer, R.; Yperman, J.; Marchal, W.; Cuypers, A.; Vandamme, D. The Effect of Pyrolysis Temperature and Feedstock on Biochar Agronomic Properties. J. Anal. Appl. Pyrolysis 2022, 168, 105728, doi:10.1016/j.jaap.2022.105728.
66. Wang, F.; Zhang, R.; Donne, S.W.; Beyad, Y.; Liu, X.; Duan, X.; Yang, T.; Su, P.; Sun, H. Co-Pyrolysis of Wood Chips and Bentonite/Kaolin: Influence of Temperatures and Minerals on Characteristics and Carbon Sequestration Potential of Biochar. Sci. Total Environ. 2022, 838, 156081, doi:10.1016/j.scitotenv.2022.156081.
67. Yang, Z.; Fang, Z.; Zheng, L.; Cheng, W.; Tsang, P.E.; Fang, J.; Zhao, D. Remediation of Lead Contaminated Soil by Biochar-Supported Nano-Hydroxyapatite. Ecotoxicol. Environ. Saf. 2016, 132, 224–230, doi:10.1016/j.ecoenv.2016.06.008.
68. Chandra, S.; Bhattacharya, J. Influence of Temperature and Duration of Pyrolysis on the Property Heterogeneity of Rice Straw Biochar and Optimization of Pyrolysis Conditions for Its Application in Soils. J. Clean. Prod. 2019, 215, 1123–1139, doi:10.1016/j.jclepro.2019.01.079.
69. Tan, Z.; Zou, J.; Zhang, L.; Huang, Q. Morphology, Pore Size Distribution, and Nutrient Characteristics in Biochars under Different Pyrolysis Temperatures and Atmospheres. J. Mater. Cycles Waste Manag. 2018, 20, 1036–1049.
70. Zhao, B.; O'Connor, D.; Zhang, J.; Peng, T.; Shen, Z.; Tsang, D.C.W.; Hou, D. Effect of Pyrolysis Temperature, Heating Rate, and Residence Time on Rapeseed Stem Derived Biochar. J. Clean. Prod. 2018, 174, 977–987.
71. López-Hernández, D.; Bates-Rondón, J. Áreas Superficiales Específicas y Parámetros Asociados En Suelos Venezolanos Con Diferentes Grados de Pedogénesis. Rev. La Fac. Agron. 2018, 26, 146–159.
72. Heilmann, S.M.; Jader, L.R.; Sadowsky, M.J.; Schendel, F.J.; von Keitz, M.G.; Valentas, K.J. Hydrothermal Carbonization of Distiller's Grains. Biomass and Bioenergy 2011, 35, 2526–2533, doi:10.1016/J.BIOMBIOE.2011.02.022.
73. Sessa, F.; Veeyee, K.F.; Canu, P. Optimization of Biochar Quality and Yield from Tropical Timber Industry Wastes. Waste Manag. 2021, 131, 341–349, doi:10.1016/j.wasman.2021.06.017.
74. Hafeez, Y.; Iqbal, S.; Jabeen, K.; Shahzad, S.; Jahan, S.; Rasul, F. Effect of Biochar Application on Seed Germination and Seedling Growth of Glycine Max (L.) Merr. under Drought Stress. Pak. J. Bot. 2017, 49, 7–13.
75. Saletnik, B.; Bajcar, M.; Zagula, G.; Czernicka, M.; Puchalski, C. Influence of Biochar and Biomass Ash Applied as Soil Amendment on Germination Rate of Virginia Mallow Seeds (Sida Hermaphrodita R.). Econtechmod 2016, 5, 71–76.
76. Khan, M.N.; Lan, Z.; Sial, T.A.; Zhao, Y.; Haseeb, A.; Jianguo, Z.; Zhang, A.; Hill, R.L. Straw and Biochar Effects on Soil Properties and Tomato Seedling Growth under Different Moisture Levels. Arch. Agron. Soil Sci. 2019, 65, 1704–1719, doi:10.1080/03650340.2019.1575510.
77. Uslu, O.S.; Babur, E.; Alma, M.H.; Solaiman, Z.M. Walnut Shell Biochar Increases Seed Germination and Early Growth of Seedlings of Fodder Crops. Agric. 2020, 10, 1–13, doi:10.3390/agriculture10100427.

Disclaimer/Publisher's Note: The statements, opinions and data contained in all publications are solely those of the individual author(s) and contributor(s) and not of MDPI and/or the editor(s). MDPI and/or the editor(s) disclaim responsibility for any injury to people or property resulting from any ideas, methods, instructions or products referred to in the content.